JACS
JOURNAL OF THE AMERICAN CHEMICAL SOCIETY
Article
pubs.acs.org/JACS

A Modular Strategy for Fully Conjugated Donor–Acceptor Block Copolymers

Sung-Yu Ku,[†,⊥,#] Michael A. Brady,[†,‡,#] Neil D. Treat,[†,‡] Justin E. Cochran,[†,§] Maxwell J. Robb,[†,§] Edward J. Kramer,[†,‡,∥,⊥] Michael L. Chabinyc,*[,†,‡,⊥] and Craig J. Hawker*[,†,‡,§,⊥]

[†] Materials Research Laboratory, [‡] Materials Department, [§] Department of Chemistry and Biochemistry, [∥] Department of Chemical Engineering, and [⊥] Mitsubishi Chemical Center for Advanced Materials, University of California, Santa Barbara, California 93106, United States

Supporting Information

ABSTRACT: A novel strategy for the synthesis of fully conjugated donor–acceptor block copolymers, in a single reaction step employing Stille coupling polymerization of end-functional polythiophene and AA + BB monomers, is presented. The unique donor–acceptor structure of these block copolymers provides a rich self-assembly behavior, with the first example of a fully conjugated donor–acceptor block copolymer having two separate crystalline domains being obtained.

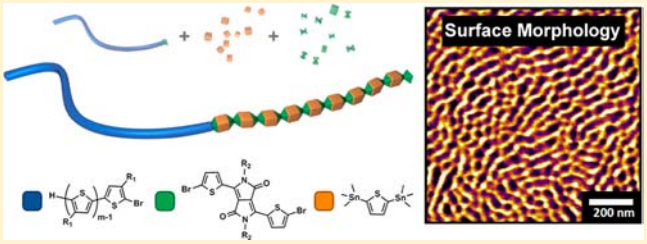

INTRODUCTION

Conjugated polymers are crucial components in the active layers of thin film electronic devices such as light-emitting diodes, field-effect transistors, and photovoltaic cells.[1] In the past decade, the power conversion efficiencies (PCEs) of polymer/fullerene bulk heterojunction (BHJ) organic photovoltaics (OPVs) have improved significantly, reaching ∼10%,[2] with advances being achieved through the development of *p*-type low bandgap polymers,[3] coupled with a better understanding of methods to control the morphology of the active layer.[4] The ideal active layer in BHJs comprises an interpenetrating donor/acceptor network that provides high interfacial area between electron-donating and electron-accepting components for efficient charge generation, while retaining continuous pathways for charge collection at the electrodes. In optimizing the nanoscale domain morphologies, annealing processes and high boiling point additives have been found to lead to enhanced PCEs.[3−5] However, due to the complexity of phase separation for multicomponent systems, coupled with major changes in morphology occurring with only minor changes in structure or processing conditions,[6] it is of great interest to develop a single material that assembles into hole- and electron-conducting domains at the nanoscale.

While a significant amount of work has been devoted to the generation of nanoscale morphologies from block copolymers, the vast majority of studies have involved one or more of the blocks being based on random copolymers or random copolymers with conjugated units attached as side chains.[7] From both an application as well as a scientific point of view, more relevant systems may be envisaged based on fully conjugated block copolymers; however, only a very limited number of fully conjugated donor–acceptor (D–A) block copolymers (C-BCPs, conjugated block copolymers) have been reported.[8,9] The paucity of examples can be attributed to the synthetic challenges in achieving the conjugated D–A block structure. One strategy involves the polycondensation reaction of AB-type monomers with end-functional P3HT. However, this method results in a complex mixture of homopolymer and C-BCP. In addition, the preparation of asymmetrical, difunctional AB-type monomers is synthetically challenging, which limits further development of D–A C-BCPs.

To address this challenge and allow for the design of C-BCPs consisting of donor and acceptor blocks for use in OPV active layers, phase-separated structures on the length scale necessary for efficient exciton dissociation (∼20 nm) and efficient charge extraction are required. These fully conjugated donor–acceptor C-BCPs must also have (a) sufficient solubility to enable solution processing, (b) a broad and intense absorption profile across the solar spectrum, and (c) a large free charge carrier mobility for facile charge transport. A new synthetic strategy for C-BCPs composed of an electron-donating poly(3-hexylthiophene) (P3HT) block and an electron-accepting poly(diketopyrrolopyrrole-terthiophene) (DPP) block is therefore presented. Significantly, the facile nature of this synthetic approach enables materials to be prepared that self-assemble into ordered morphologies on multiple length scales, including that of exciton diffusion, and enables understanding of C-BCP structure–processing–performance relationships in OPV devices.

RESULTS AND DISCUSSION

To facilitate access to C-BCPs, a new synthetic strategy based on the Stille coupling of a mixture of bromine-terminated

Received: July 27, 2012
Published: September 13, 2012

   dx.doi.org/10.1021/ja307431k | *J. Am. Chem. Soc.* 2012, 134, 16040–16046

P3HT and AA + BB monomers was developed. By employing a monofunctional P3HT block, copolymerization with AA/BB monomers would then give a block copolymer in which the P3HT blocks are connected to a DPP block by a condensation reaction. However, it should be noted that this strategy could result in a mixture of di- and triblock copolymers, since quantitative end capping of both chain ends of the P3HT block is unlikely. To exemplify this new approach, we report the synthesis and characterization of regioregular poly(3-hexylthiophene)-*block*-poly(diketopyrrolopyrrole-terthiophene), P3HT-*b*-DPP. In our C-BCP system, the P3HT segment serves as the electron donor, and the DPP block serves as the electron acceptor.[10] The advantage of this strategy is its modularity with respect to preparation of a wide variety of stable AA and BB monomers. By varying the AA and BB monomers, tailoring of the C-BCP energy levels is possible, while also providing high-purity C-BCPs on a reasonable scale.

The starting P3HT block was first prepared by Grignard metathesis polymerization, following the procedure developed by McCullough et al. (see the Supporting Information).[11] This method leads to well-defined P3HT with controlled molecular weights, polydispersity indices (PDIs) of ∼1.1, and a single bromo chain end (P3HT-Br). Conversely, the fused ring dibromo-1,4-diketopyrrolo[3,4-*c*]pyrrole (DPP) unit serves as the BB monomer and can be prepared in three steps, as described previously.[12] The C-BCPs are then synthesized in a single step from a mixture of 2,5-bis(trimethylstannyl)-thiophene (1.0 equiv of AA monomer), DPP (1.0 equiv of BB monomer), and varying amounts of P3HT-Br (8−20 mol % or ca. 0.01−0.05 equiv) under microwave irradiation, using $Pd_2(dba)_3$/P(*o*-tolyl)$_3$ as the catalyst (Scheme 1). The C-BCPs

Scheme 1. Utilizing Stille Coupling Polymerization of End-Functional P3HT and AA + BB Monomers, a Novel Strategy for the Synthesis of Fully Conjugated Block Copolymers, Such as P3HT-*b*-DPP, is Presented

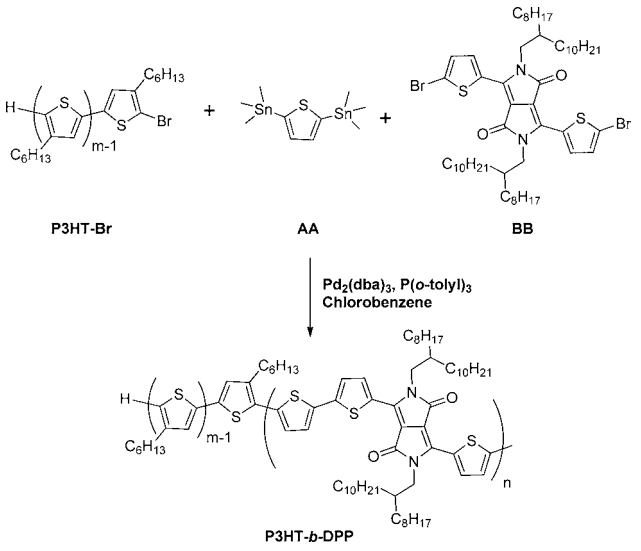

can be easily purified from homopolymer contaminants by Soxhlet extraction and characterized by ^{1}H NMR, UV−vis, and gel permeation chromatography (GPC). As a control sample, poly(diketopyrrolopyrrole-terthiophene), DPPT homopolymer, was synthesized from the AA and BB monomers, 2,5-bis(trimethylstannyl)-thiophene and DPP, respectively, under Stille-coupling polymerization in the absence of the chain-terminating P3HT units (see the Supporting Information).

Due to the condensation nature of the polymerization process, it was critical to fully characterize the reaction product and to demonstrate both block copolymer formation and the absence of significant homopolymer contamination. Initial analysis by ^{1}H NMR spectroscopy provided evidence for block copolymer synthesis, with the NMR spectrum for the product showing distinct resonances for both the P3HT and DPP units. In addition, the disappearance of peaks resulting from the bromo-chain end of the P3HT block was fully consistent with C-BCP formation (Figure 1). For example, two triplets are

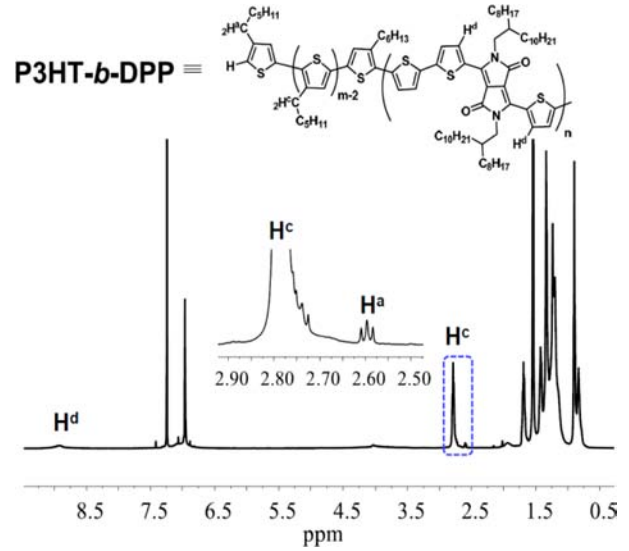

Figure 1. ^{1}H NMR (600 MHz) spectrum for a representative C-BCP, P3HT$_{87}$-*b*-DPP$_{13}$.

observed in the ^{1}H NMR spectrum of the starting P3HT-Br (see the Supporting Information) at 2.55 ppm (α-methyl protons of the terminal bromo-hexylthiophene; H^b) and 2.60 ppm (α-methyl protons of the terminal H-hexylthiophene; H^a);[13] after reaction with DPP and 2,5-bis(trimethylstannyl)-thiophene, the triplet at 2.55 ppm is absent, and only the peaks at 2.60 ppm, representing the α-methyl protons of the terminal hexylthiophene (H^a), are present. This change in the ^{1}H NMR spectra is fully consistent with efficient transformation of the bromo-chain end to an aryl-derivative during formation of the P3HT-*b*-DPP C-BCP. Integration of distinct resonances for each block, including the α-methylene protons of P3HT (2.80 ppm; H^c) and the peak corresponding to the aromatic proton of the thiophene adjacent to the diketopyrrolopyrrole unit (8.92 ppm; H^d), allowed the relative sizes of the two blocks to be determined based on the accurate molecular weight for the starting, well-defined P3HT derivatives. From this analysis, the molecular weights, PDIs, and compositions of polymers prepared in this work could be established and are summarized in Table 1.

By having demonstrated that both P3HT and DPP units are present in the product, it was essential to confirm purity and the absence of homopolymer contamination. Gel permeation chromatography coupled with both refractive index (RI) and UV detectors gave critical insight on the absence of significant homopolymer contamination. Figure 2a shows a comparison of the GPC RI detector traces for the starting P3HT-Br block (M_n = 8100 g/mol) and the purified P3HT$_{87}$-*b*-DPP$_{13}$ C-BCP. For

dx.doi.org/10.1021/ja307431k | J. Am. Chem. Soc. 2012, 134, 16040−16046

Table 1. Molar Ratios of Repeat Units, Molecular Weights, and PDIs for P3HT- and DPP-Based Polymers

polymer	molar ratio of repeat unit	M_n (g/mol)	M_w (g/mol)	PDI
P3HT-Br (8 k)	100/0	8100	8700	1.07
DPPT	0/100	26 300	60 500	2.29
P3HT(8 k)$_{87}$-*b*-DPP$_{13}$	87/13	37 200	69 400	1.86
P3HT(8 k)$_{63}$-*b*-DPP$_{37}$	63/37	44 200	84 500	1.91
P3HT-Br (19 k)	100/0	18 900	22 600	1.19
P3HT(19 k)$_{85}$-*b*-DPP$_{15}$	85/15	66 300	104 800	1.58
P3HT(19 k)$_{72}$-*b*-DPP$_{28}$	72/28	70 400	133 500	1.89

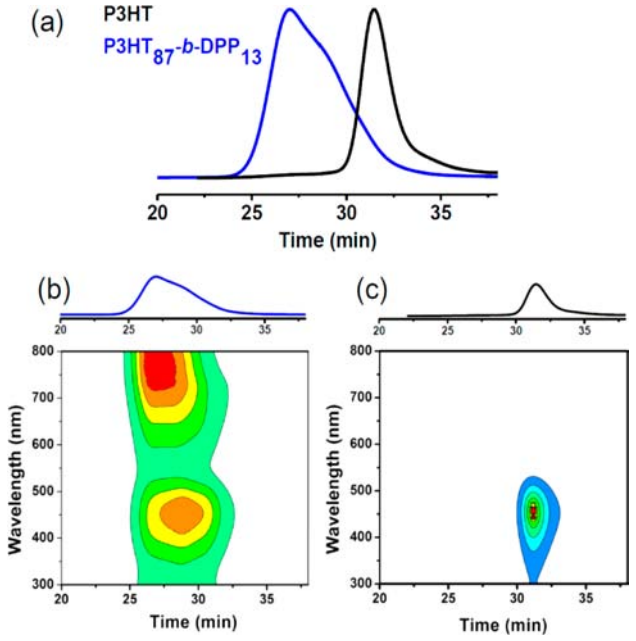

Figure 2. (a) GPC traces for P3HT-Br (8 k) and P3HT$_{87}$-*b*-DPP$_{13}$ based on an RI detector; GPC traces for (b) P3HT$_{87}$-*b*-DPP$_{13}$ and (c) P3HT-Br (8 k) based on a UV detector.

the C-BCP, only minor tailing is observed, corresponding to a similar molecular weight as the P3HT-Br. This shoulder may originate from either lower molecular weight block copolymer or from the presence of residual P3HT or DPPT homopolymers. In order to address this concern, GPC contour plots based on a photodiode UV detector were examined for the P3HT$_{87}$-*b*-DPP$_{13}$ C-BCP (Figure 2b) and compared to those of the starting P3HT-Br block (Figure 2c). While the P3HT shows only a narrow absorption, from 350 to 550 nm at 31 min, the C-BCP shows two absorbances at 350−550 and 550−800 nm, with the long wavelength absorbance also occurring at the high retention times. This strongly suggests that the low molecular weight tail contains both P3HT and DPP segments and is primarily C-BCP with little P3HT homopolymer contamination. As a control, a physical blend of P3HT and DPPT homopolymers was examined and clearly demonstrated two distinct absorption regions at different retention times (see the Supporting Information).

One attractive feature of this modular synthetic strategy is the high degree of flexibility afforded over the structure and chemical composition of the resulting C-BCPs. For example, with the total number of AA + BB monomers held equal, the molecular weight and relative block lengths of the C-BCP can be tailored by varying the molecular weight and amount of the starting P3HT block. High molecular weight C-BCPs (e.g., P3HT$_{63}$-*b*-DPP$_{37}$) were synthesized by reducing the mole percent of P3HT-Br in the reaction mixture from 20 to 8 mol %, and conversely, increasing the amount of P3HT-Br resulted in effective lowering of the DPP block length (e.g., P3HT$_{87}$-*b*-DPP$_{13}$). In addition, the length of the P3HT block can be easily controlled by employing starting P3HT units of different molecular weight (M_n = 18 900 g/mol).

While this strategy is very useful for controlling the relative molecular weights and mole percentages of each block, the real power of this strategy is the ability to easily modify the chemical structure of the blocks. Both the P3HT and DPP blocks can be exchanged for other repeat unit structures, with well-defined block copolymers being obtained in each case. To demonstrate this versatility, poly(3-ethylhexylthiophene) (P3EHT) and/or different acceptors, such as diketopyrrolo[3,4-*c*]pyrrole containing furan (DPPF), were used to synthesize alternative examples of C-BCPs (Figure 3). For these acceptor systems

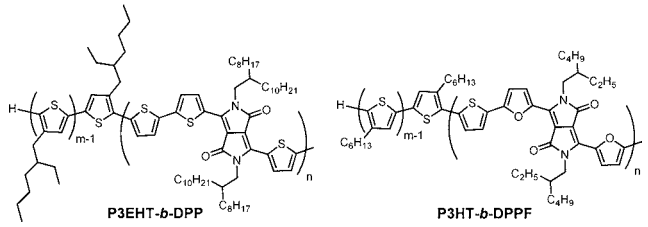

Figure 3. Alternative C-BCPs prepared using the modular synthetic strategy described in this work: P3EHT-*b*-DPP and P3HT-*b*-DPPF.

with 8 mol % of P3EHT-Br (8 k) or P3HT-Br (21 k), copolymerization gave P3EHT-*b*-DPP (M_n = 25 400 g/mol) or P3HT-*b*-DPPF (M_n = 109 000 g/mol), respectively, with the GPC results summarized in Table 2.

Table 2. Molecular Characteristics for Alternative C-BCPs, Demonstrating Versatility in Both the Starting Homopolymer and AA/BB Monomers

polymer	molar ratio of repeat unit	M_n (g/mol)	M_w (g/mol)	PDI
P3EHT-Br (8 k)	100/0	8600	12 600	1.46
P3EHT(8 k)$_{58}$-*b*-DPP$_{42}$	58/42	25 400	53 600	2.10
P3HT-Br (21 k)	100/0	21 500	26 900	1.24
P3HT(21 k)$_{62}$-*b*-DPPF$_{38}$	62/38	109 000	162 000	1.48

The inherent versatility in this synthetic approach then allows the physical properties of the block copolymers to be tailored. As an initial example, broad optical absorbance is highly desirable for OPV applications, and the UV−vis absorption spectrum of P3HT-*b*-DPP, measured in dichlorobenzene solution and as a thin film (Figure 4a), shows a broad absorption profile over the UV−visible region. For the solution spectrum, two specific absorption peaks, resulting from the P3HT and DPP blocks, were observed at approximately 450 and 750 nm, respectively. The thin film spectrum is significantly red-shifted, as compared to the solution spectrum, indicating that chain ordering is enhanced during casting.

dx.doi.org/10.1021/ja307431k | J. Am. Chem. Soc. 2012, 134, 16040−16046

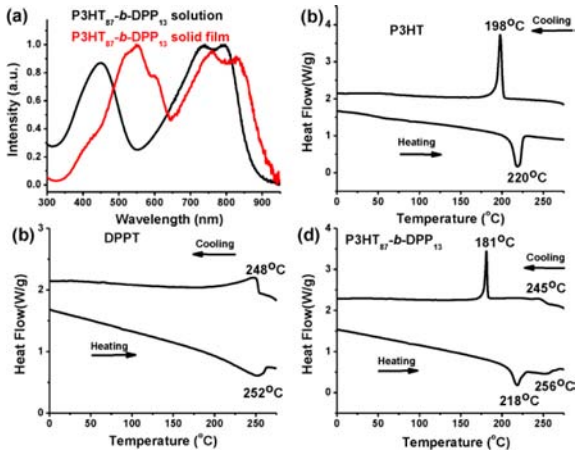

Figure 4. (a) UV−vis spectra of P3HT$_{87}$-*b*-DPP$_{13}$ in solution and solid film; DSC for (b) P3HT, (c) DPPT, and (d) P3HT$_{87}$-*b*-DPP$_{13}$.

The potential for chain ordering in this system is particularly intriguing given the semicrystalline nature of both parent P3HT and DPP homopolymers. To investigate the influence of covalently linking two semicrystalline chains, the thermal transitions of the block copolymers were compared to those for the homopolymers as well as a control system, the corresponding physical blend. Significantly, the P3HT$_{87}$-*b*-DPP$_{13}$ C-BCP shows melting transitions at 218 and 256 °C (Figure 4d), with the lower T_m corresponding to the P3HT segment and the higher T_m to the DPP segment. These transitions are fully consistent with the respective homopolymers, as P3HT (M_n = 8100 g/mol) gives a single endothermic peak on heating at 220 °C and a crystallization transition at 198 °C upon cooling (Figure 4b), while the DPPT homopolymer shows an endothermic peak on heating at 252 °C and a crystallization transition at 248 °C upon cooling (Figure 4c). This close correspondence between the melting transitions of the block copolymer and the respective homopolymers was also observed for all other diblock copolymers prepared in this work.

This retention of crystallinity for both blocks is surprising given the molecular requirements for crystalline order and prompted a thorough investigation of the morphology of P3HT-*b*-DPP thin films. Thin films of P3HT$_{87}$-*b*-DPP$_{13}$ were therefore cast from 1,2-dichlorobenzene and analyzed by atomic force microscopy (AFM) after annealing at 200, 225, and 265 °C (Figure 5) with the temperatures being chosen based on the melting transitions for the respective copolymer crystalline regions. At intermediate temperatures of 200 and 225 °C, microphase separation is observed; however, well-defined morphologies are not apparent (Figure 5b and c, respectively). This is in direct contrast to the sample annealed at 265 °C, which is above the melting transition for both the P3HT and DPP crystallites. In this case, well-defined and distinct domains are observed that can be attributed to nanoscale self-assembly of the P3HT and DPP segments (Figure 5d). This nanoscale morphology may be caused by several factors, including liquid-state aggregation[14] and thermodynamically driven phase separation,[15] which is a function of both Flory−Huggins interaction and Meier-Saupe parameters coupled with the ability for each block to participate in crystalline and amorphous regions.[16]

While AFM reveals the presence of nanoscale domains, it does not provide information about molecular ordering. To

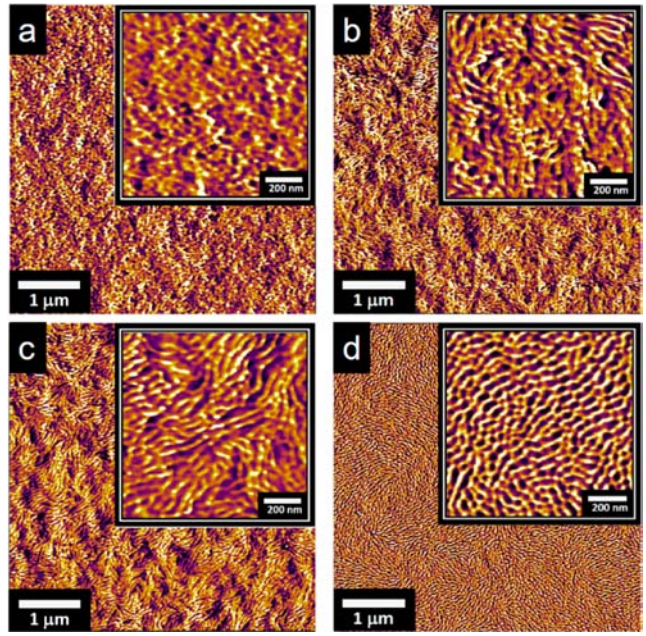

Figure 5. AFM phase images of P3HT$_{87}$-*b*-DPP$_{13}$: (a) as-cast and (b−d) annealed at (b) 200 °C, (c) 225 °C, and (d) 265 °C; the AFM inset box is 1 μm × 1 μm in size.

investigate the C-BCP crystallite structure and favored crystalline domain orientations, these C-BCP thin films were analyzed by grazing-incidence wide-angle X-ray scattering (GIWAXS). As a representative example, the crystallinity of the C-BCP P3HT$_{87}$-*b*-DPP$_{13}$ was found to increase when annealed at 200 °C, as compared to the as-cast film, and the crystallites are dominantly arranged in an edge-on orientation. GIWAXS data for P3HT$_{87}$-*b*-DPP$_{13}$, as-cast (Figure 6a) and after annealing at 200 °C (Figure 6b), clearly indicate the effect of annealing and the high degree of crystallinity for both the P3HT and DPP segments. High-resolution specular X-ray

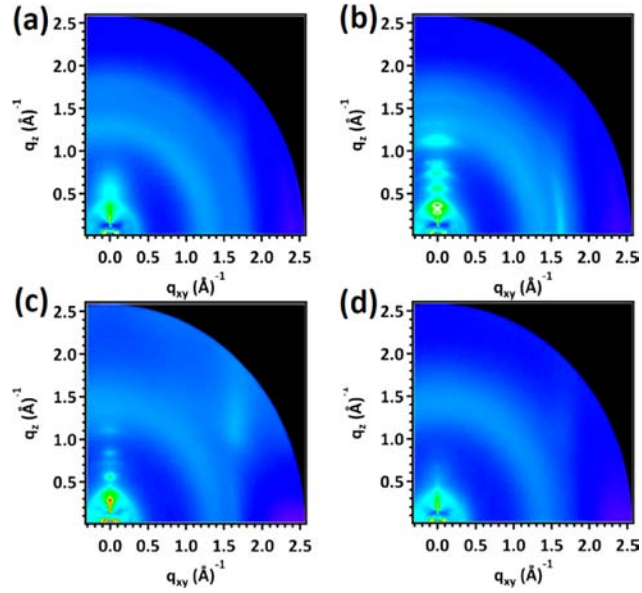

Figure 6. (a) GIWAXS of as-cast P3HT$_{87}$-*b*-DPP$_{13}$; (b−d) GIWAXS of P3HT$_{87}$-*b*-DPP$_{13}$ annealed at (b) 200 °C, (c) 225 °C, and (d) 265 °C.

dx.doi.org/10.1021/ja307431k | J. Am. Chem. Soc. 2012, 134, 16040−16046

diffraction results (Figure 7) indeed reveal the presence of crystalline P3HT and DPP regions when the thin film is

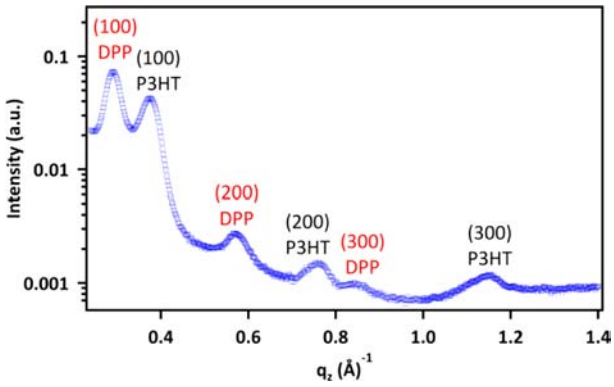

Figure 7. Specular X-ray diffraction for P3HT$_{87}$-*b*-DPP$_{13}$, annealed at 200 °C, where the (*h*00) peaks for both P3HT and DPP segments are indexed.

annealed below both melting temperatures (200 °C). By comparing these data to diffraction results from the homopolymers, the identification of three orders of diffraction for both P3HT and DPP in the C-BCP films was possible. GIWAXS analysis for P3HT$_{87}$-*b*-DPP$_{13}$ thin films annealed at 225 and 265 °C (Figure 6c and d, respectively) shows that annealing above the melting transition of each block and cooling leads to the disappearance of the respective diffraction peaks. When cooled from the melt temperature of P3HT (225 °C), P3HT$_{87}$-*b*-DPP$_{13}$ films exhibit significant crystalline order but only in the DPP domains. Alternatively, cooling from the melt temperature of DPP (265 °C) results in the loss of significant crystalline order for both blocks.

It is of major interest to note that increasing the annealing temperature eventually results in significantly enhanced domain ordering on the ∼30 nm length scale while causing a loss in ordering on the smaller, crystallite length scale. For example, the P3HT$_{87}$-*b*-DPP$_{13}$ film annealed at 265 °C shows distinct lamellar domains while both blocks are amorphous. The length scale corresponding to these lamellar domain structures, with characteristic distances of ∼30 nm, is correlated to the expected molecular dimensions of the block copolymers and, more importantly from an OPV perspective, expected exciton diffusion lengths. Additionally, the implication of lamellar domain ordering perpendicular to the film plane is a particularly important feature of the observed domain structure, representing the ideal OPV morphology. It should be noted that, for the control system where the two homopolymers are blended in the same weight ratio as the corresponding block copolymer, gross macrophase separation is observed with no significant ordering (see the Supporting Information). These initial AFM and X-ray scattering experiments indicate the importance of covalently attaching the semicrystalline blocks for the formation of a well-ordered, nanoscale morphology. To the best of our knowledge, this is also the first example to show that two distinct semicrystalline, nanoscale domains can be present in a fully conjugated D−A block copolymer system.

The assembly of the C-BCP into an ordered domain structure at temperatures above the melting transition of each block may be due to Flory−Huggins interaction energies between P3HT and DPP segments. However, one must also consider the roles that P3HT block and DPP block crystallization play in formation of these domains. GIWAXS results clearly indicate that both blocks participate in crystalline regions; chains assemble into lamellae in the alkyl stacking direction, largely perpendicular to the substrate, and into sheets in the π-stacking direction, largely parallel to the substrate plane. Specifically, three orders of diffraction from (*h*00) planes of both P3HT and DPP are observed in the out-of-plane direction, q_z, while the in-plane direction, q_{xy}, contains a reflection from a length scale characteristic of stacking perpendicular to the conjugation plane of the chains. Within the larger lamellar domains, these crystallites exist along with amorphous regions of the C-BCP, and their formation likely has a significant impact on the assembly of each block segment into the observed domain structure. Currently, how these crystalline regions are distributed within the domains and how they affect the donor−acceptor interface, intradomain structure, and microphase separation process are under investigation. Nonetheless, it is evident that the covalent bond between the donor and acceptor blocks has a significant effect on film morphology, promoting microphase separation and introducing structure on the order of 30 nm, without significantly interfering with the crystallinity of the P3HT and DPP polymer blocks. This covalent bond leads to highly oriented crystallites and ordered domain morphologies, as compared to the lower orientational order of crystallites and lack of domain ordering when P3HT and DPP homopolymers are blended and cast (see the Supporting Information).

■ CONCLUSION

In this report, we present a modular route for synthesizing fully conjugated donor−acceptor block copolymers based on the condensation of monofunctionalized, bromo-terminated polythiophenes with AA + BB monomers. Significant structural versatility is inherent in this strategy, which allows the self-assembly behavior of these novel C-BCPs to be studied in detail. The covalent bond between P3HT and DPP not only allows for an ordered microstructure on multiple length scales, but it also leads to self-assembled, semicrystalline domains on the length scale of exciton diffusion. The interplay between this dual crystallization of the rod−rod block copolymer and its nanoscale phase separation is a topic of further study.

■ EXPERIMENTAL SECTION

General Methods. All reagents from commercial sources were used without further purification. Flash chromatography was performed using silica gel (particle size 40−63 μm). *N*,*N*-dimethylformamide (DMF), tetrahydrofuran (THF), and dichloromethane (DCM) were purchased from Fisher Scientific. All compounds were characterized by ^{1}H NMR (600 MHz) using Varian 600 instruments, with the solvent signal as internal reference and the spectra being acquired at room temperature. Samples were introduced using a direct insertion probe. Microwave reactions were performed using a Biotage microwave reactor. For polymer molecular weight determination, polymer samples were dissolved in chloroform at a concentration of 1 mg/mL, briefly heated, and then allowed to return to room temperature prior to filtering through a 0.45 μm filter. Gel permeation chromatography (GPC) was performed in chloroform ($CHCl_3$) on a Waters 2690 separation module equipped with a Waters 2414 refractive index detector and a Waters 2996 photodiode array detector. Molecular weights were calculated relative to linear PS standards. Differential scanning calorimetry (DSC) was performed under a nitrogen atmosphere at a heating rate of 10 °C/min. Atomic force microscopy (AFM) was conducted on an Asylum Research MFP 3D AFM, using NanoWorld Pointprobe Al-coated, noncontact mode Si cantilevers, with a resonant frequency of 190 kHz and a spring

constant of 48 N/m. Two-dimensional (2D) grazing-incidence wide-angle X-ray scattering (GIWAXS) measurements were performed at the Stanford Synchrotron Radiation Lightsource (SSRL) on beamline 11-3, with a MAR345 image plate area detector, at 12.7 keV incident photon energy, and at incident angles of 0.10−0.12°. Thin film illumination occurred in a helium atmosphere to minimize X-ray beam damage. Specular X-ray diffraction was collected at SSRL beamline 2-1 with an 8 keV incident photon energy.

Synthesis of P3HT-Br. A dried Schlenk flask equipped with a magnetic stir bar was charged with 2,5-dibromo-3-hexylthiophene (1.53 g, 4.71 mmol) in 50 mL of dry THF under argon. A solution of *t*-butylmagnesium chloride in THF (2.35 mL, 4.71 mmol, 2.00 M) was added, and the mixture was heated for 1.5 h at 40 °C. After cooling to room temperature, nickel(II)-[bis(diphenylphosphino)propane]-chloride, Ni(dppp)Cl_2 (25 mg, 0.047 mmol) was quickly added, and the reaction mixture was stirred for 30 min, quenched with 3 mL of hydrochloric acid (10%), and then poured into methanol. The crude product was filtered off and purified by subsequent Soxhlet extraction with methanol, hexane, and acetone to yield P3HT-Br polymer (270 mg, 35% yield). ^{1}H NMR ($CDCl_3$, 600 MHz): δ 6.96 (m, br), 2.78 (m, br), 1.68 (m, br), 1.34 (m, br), 1.32 (m, br), 1.31 (m, br), 0.89 (m, br). GPC ($CHCl_3$): M_n = 8100 g/mol; M_w = 8700 g/mol; PDI = 1.07. The molecular weight of polythiophene can be calculated by analysis of the α-methyl protons of hexylthiophene from the P3HT-Br NMR spectrum. The integration of H^a/H^c is equal to $1/(m-2)$. The molecular weight of P3HT-Br is estimated as ∼3400 g/mol.

Synthesis of DPPT Homopolymer. A mixture of 2,5-bis-(trimethylstannyl)thiophene (102.4 mg, 0.25 mmol), DPP (254.8 mg, 0.25 mmol), $Pd_2(dba)_3$ (4.5 mg, 0.005 mmol), and P(*o*-tolyl)$_3$ (6.1 mg, 0.02 mmol) was placed in a 10 mL microwave vial and sealed. Dry chlorobenzene (4 mL) was injected in the vial, and the mixture was sparged with argon for 20 min and then heated at 120 °C for 3 min, 150 °C for 3 min, and finally 180 °C for 50 min under microwave irradiation. The reaction mixture was allowed to cool to 55 °C, and then, 30 mL of *o*-DCB was added to dissolve any precipitated polymer; the mixture was eluted with chloroform through a silica plug. After precipitation into methanol (250 mL), the product was purified by Soxhlet extraction with methanol and acetone to yield the desired polymer, DPPT (230 mg, 97% yield), as a dark solid. ^{1}H NMR ($CDCl_3$, 600 MHz): δ 8.92 (m, br), 7.41 (m, br), 7.06 (m, br), 4.02 (m, br), 1.93 (m, br), 1.22 (m, br), 0.86 (m, br). GPC ($CHCl_3$): M_n = 26 300 g/mol; M_w = 60 500 g/mol; PDI = 2.29.

Synthesis of P3HT-*b*-DPP Block Copolymer. A mixture of P3HT-Br (8 kDa; GPC) (100 mg, 3400 g/mol (NMR), 0.03 mmol), 2,5-bis(trimethylstannyl)thiophene (61.4 mg, 0.15 mmol), DPP (152.8 mg, 0.15 mmol), $Pd_2(dba)_3$ (2.7 mg, 0.003 mmol), and P(*o*-tolyl)$_3$ (3.7 mg, 0.012 mmol) was placed in a 10 mL microwave vial and sealed. Dry chlorobenzene (4 mL) was injected into the vial; the mixture was sparged with argon for 20 min and then heated at 120 °C for 3 min, 150 °C for 3 min, and finally 180 °C for 50 min under microwave irradiation. The reaction mixture was allowed to cool to 55 °C, and then, 30 mL of *o*-DCB was added to dissolve any precipitated polymer; the mixture was eluted with chloroform through a silica plug. After precipitation into methanol (250 mL), the product was purified by Soxhlet extraction with methanol, hexane, and acetone to yield the desired polymer, $P3HT_{87}$-*b*-DPP_{13} (220 mg, 91% yield), as a dark solid. ^{1}H NMR ($CDCl_3$, 600 MHz): δ 8.92 (m, br), 6.97 (m, br), 4.02 (m, br), 2.80 (m, br), 1.95 (m, br), 1.72 (m, br), 1.51 (m, br), 1.43 (m, br), 1.35 (m, br), 0.93 (m, br), 0.85 (m, br). GPC ($CHCl_3$): M_n = 37 200 g/mol; M_w = 69 400 g/mol; PDI = 1.86.

Synthesis of P3EHT-*b*-DPP Block Copolymer. A mixture of P3EHT-Br (8 kDa; GPC) (60 mg, 5000 g/mol (NMR), 0.012 mmol), 2,5-bis(trimethylstannyl)thiophene (61.4 mg, 0.15 mmol), DPP (152.8 mg, 0.15 mmol), $Pd_2(dba)_3$ (2.7 mg, 0.003 mmol), and P(*o*-tolyl)$_3$ (3.7 mg, 0.012 mmol) was placed in a 10 mL microwave vial and sealed. Dry chlorobenzene (4 mL) was injected into the vial, and the mixture was sparged with argon for 20 min. The mixture was then heated at 120 °C for 3 min, 150 °C for 3 min, and finally 180 °C for 50 min under microwave irradiation. The reaction mixture was allowed to cool to 55 °C, and then 30 mL of *o*-DCB was added to dissolve any precipitated polymer; the mixture was eluted with chloroform through a silica plug. After precipitation into methanol (250 mL), the product was dried to yield the desired polymer, $P3EHT_{58}$-*b*-DPP_{42} (200 mg, 95% yield), as a dark solid. ^{1}H NMR ($CDCl_3$, 600 MHz): δ 8.89 (m, br), 6.91 (m, br), 4.03 (m, br), 2.75 (m, br), 1.94 (m, br), 1.70 (m, br), 1.51 (m, br), 1.43 (m, br), 1.35 (m, br), 0.93 (m, br), 0.88 (m, br). GPC ($CHCl_3$): M_n = 25 400 g/mol; M_w = 53 600 g/mol; PDI = 2.10.

Synthesis of P3HT-*b*-DPPF Block Copolymer. A mixture of P3HT-Br (21 kDa; GPC) (80 mg, 5000 g/mol (NMR), 0.016 mmol), 2,5-bis(trimethylstannyl)thiophene (81.9 mg, 0.20 mmol), DPPF (130.0 mg, 0.20 mmol), $Pd_2(dba)_3$ (3.7 mg, 0.004 mmol), and P(*o*-tolyl)$_3$ (4.9 mg, 0.016 mmol) was placed in a 10 mL microwave vial and sealed. Dry chlorobenzene (4 mL) was injected into the vial, and the mixture was sparged with argon for 20 min. The mixture was then heated at 120 °C for 3 min, 150 °C for 3 min, and finally 180 °C for 50 min under microwave irradiation. The reaction mixture was allowed to cool to 55 °C, and then 30 mL of *o*-DCB was added to dissolve any precipitated polymer; the mixture was eluted with chloroform through a silica plug. After precipitation into methanol (250 mL), the product was purified by Soxhlet extraction with methanol, hexane, and acetone to yield the desired polymer, $P3HT_{62}$-*b*-$DPPF_{38}$ (165 mg, 85% yield), as a dark solid. ^{1}H NMR ($CDCl_3$, 600 MHz): δ 8.81 (m, br), 6.90 (m, br), 4.83 (m, br), 2.73 (m, br), 2.05 (m, br), 1.72 (m, br), 1.51 (m, br), 1.43 (m, br), 1.35 (m, br), 0.95 (m, br), 0.86 (m, br). GPC ($CHCl_3$): M_n = 109 000 g/mol; M_w = 162 000 g/mol; PDI = 1.48.

■ ASSOCIATED CONTENT

Ⓢ Supporting Information

Detailed experimental procedures, characterization of all compounds, thin film preparation, and GPC, DSC, AFM, and GIWAXS studies. This material is available free of charge via the Internet at http://pubs.acs.org.

■ AUTHOR INFORMATION

Corresponding Author

mchabinyc@engineering.ucsb.edu; hawker@mrl.ucsb.edu

Author Contributions

[#]These authors contributed equally.

Notes

The authors declare no competing financial interest.

■ ACKNOWLEDGMENTS

This work was partially supported by the Mitsubishi Chemical Center for Advanced Materials (S.K. and E.J.K.) at UCSB and the NSF SOLAR program (CHE-1035292) (M.A.B., N.D.T., M.L.C., and C.J.H.). Portions of this research were carried out at the SSRL, a national user facility operated by Stanford University on behalf of the U.S. Department of Energy, Office of Basic Energy Sciences, as well as at the MRL Central Facilities, which are supported by the MRSEC Program of the NSF under award no. DMR-1121053 (M.A.B., J.E.C., E.J.K., M.L.C., and C.J.H.). M.A.B. would like to acknowledge funding from NSF and California Nanosystems Institute Graduate Research Fellowships. M.J.R. thanks the DOE Office of Science for a Graduate Fellowship (DOE SCGF).

■ REFERENCES

(1) (a) Günes, S.; Neugebauer, H.; Sariciftci, N. S. *Chem. Rev.* **2007**, *107*, 1324. (b) Thompson, B. C.; Fréchet, J. M. J. *Angew. Chem., Int. Ed.* **2008**, *47*, 58.

(2) Green, M. A; Emery, K.; Hishikawa, Y.; Warta, W.; Dunlop, E. D. *Prog. Photovoltaics* **2012**, *20*, 12.

(3) Peet, J.; Kim, J. Y.; Coates, N. E.; Ma, W. L.; Moses, D.; Heeger, A. J.; Bazan, G. C. *Nat. Mater.* **2007**, *6*, 497.

(4) (a) van Bavel, S. S.; Bärenklau, M.; de With, G.; Hoppe, H.; Loos, J. *Adv. Funct. Mater.* **2010**, *20*, 1458. (b) Brabec, C. J.; Gowrisanker, S.; Halls, J. J. M.; Laird, D.; Jia, S.; Williams, S. P. *Adv. Mater.* **2010**, *22*, 3839. (c) Brady, M. A.; Su, G. M.; Chabinyc, M. L. *Soft Matter* **2011**, *7*, 11065.
(5) (a) Liang, Y.; Xu, Z.; Xia, J.; Tsai, S. T.; Wu, Y.; Li, G.; Ray, C.; Yu, L. *Adv. Mater.* **2010**, *22*, E135. (b) Rogers, J. T.; Schmidt, K.; Toney, M. F.; Bazan, G. C.; Kramer, E. J. *J. Am. Chem. Soc.* **2012**, *134*, 2884.
(6) Treat, N. D.; Brady, M. A.; Smith, G.; Toney, M. F.; Kramer, E. J.; Hawker, C. J.; Chabinyc, M. L. *Adv. Energy Mater.* **2011**, *1*, 82.
(7) (a) Scherf, U.; Gutacker, A.; Koenen, N. *Acc. Chem. Res.* **2008**, *41*, 1086. (b) Scherf, U.; Adamczyk, S.; Gutacker, A.; Koenen, N. *Macromol. Rapid Commun.* **2009**, *30*, 1059. (c) He, M.; Qiu, F.; Lin, Z. *J. Mater. Chem.* **2011**, *21*, 17039. (d) Tseng, Y. C.; Darling, S. B. *Polymers* **2010**, *2*, 470. (e) Sommer, M.; Lang, A. S.; Thelakkat, M. *Angew. Chem., Int. Ed.* **2008**, *47*, 7901. (f) Sommer, M.; Huettner, S.; Thelakkat, M. *J. Mater. Chem.* **2010**, *20*, 10788. (g) Hadziioannou, G. *MRS Bull.* **2002**, *27*, 456. (h) Topham, P. D.; Parnell, A. J.; Hiorns, R. C. *J. Polym. Sci., Part B: Polym. Phys.* **2011**, *49*, 1131. (i) Yu, X.; Yang, H.; Wu, S.; Geng, Y.; Hang, Y. *Macromolecules* **2012**, *45*, 266. (j) Bates, F. S.; Hillmyer, M. A.; Lodge, T. P.; Bates, C. M.; Delaney, K. T.; Fredrickson, G. H. *Science* **2012**, *336*, 434. (k) Bang, J.; Jeong, U.; Ryu, D. Y.; Russell, T. P.; Hawker, C. J. *Adv. Mater.* **2009**, *21*, 4769. (l) Xu, T.; Stevens, J.; Villa, J. A.; Goldbach, J. T.; Guarim, K. W.; Black, C. T.; Hawker, C. J.; Russell, T. P. *Adv. Funct. Mater.* **2003**, *13*, 698−702. (m) Jeong, U. Y.; Kim, H. C.; Rodriguez, R. L.; Tsai, I. Y.; Stafford, C. M.; Kim, J. K.; Hawker, C. J.; Russell, T. P. *Adv. Mater.* **2002**, *14*, 274.
(8) (a) Verduzco, R.; Botiz, I.; Pickel, D. L.; Kilbey, S. M.; Hong, K.; Dimasi, E.; Darling, S. B. *Macromolecules* **2011**, *44*, 530. (b) Izuhara, D.; Swager, T. M. *Macromolecules* **2011**, *44*, 2678. (c) Woody, K. B.; Leever, B. J.; Durstock, M. F.; Collard, D. M. *Macromolecules* **2011**, *44*, 4690. (d) Sommer, M.; Komber, H.; Huettner, S.; Mulherin, R.; Kohn, P.; Greenham, N. C.; Huck, W. T. S. *Macromolecules* **2012**, *45*, 4142.
(9) (a) Mulherin, R. C.; Jung, S.; Huettner, S.; Johnson, K.; Kohn, P.; Sommer, M.; Allard, S.; Scherf, U.; Greenham, N. C. *Nano Lett.* **2011**, *11*, 4846. (b) Lai, Y.; Ohshimizu, K.; Takahashi, A.; Hsu, J.; Higashihara, T.; Ueda, M.; Chen, W.-C. *J. Polym. Sci., Part A: Polym. Chem.* **2011**, *49*, 2577−2587. (c) Ohshimizu, K.; Takahashi, A.; Higashihara, T.; Ueda, M. *J. Polym. Sci., Part A: Polym. Chem.* **2011**, *49*, 2709−2714. (d) Yuan, M.; Rice, A. H.; Luscombe, C. K. *J. Polym. Sci., Part A: Polym. Chem.* **2011**, *49*, 701−711.
(10) Zhang, X.; Richter, L. J.; DeLongchamp, D. M.; Kline, R. J.; Hammond, M. R.; McCulloch, I.; Heeney, M.; Ashraf, R. S.; Smith, J. N.; Anthopoulos, T. D.; Schroeder, B.; Geerts, Y. H.; Fischer, D. A.; Toney, M. F. *J. Am. Chem. Soc.* **2011**, *133*, 15073.
(11) Iovu, M. C.; Sheina, E. E.; Gil, R. R.; McCullough, R. D. *Macromolecules* **2005**, *38*, 8649.
(12) (a) Li, Y.; Singh, S. P.; Sonar, P. *Adv. Mater.* **2010**, *22*, 4862. (b) Woo, C. H.; Beaujuge, P. M.; Holcombe, T. W.; Lee, O. P.; Fréchet, J. M. J. *J. Am. Chem. Soc.* **2010**, *132*, 15547.
(13) Verswyvel, M.; Monnaie, F.; Koeckelberghs, G. *Macromolecules* **2011**, *44*, 9489.
(14) Park, Y. D.; Park, J. K.; Seo, J. H.; Yuen, J. D.; Lee, W. H.; Cho, K.; Bazan, G. C. *Adv. Energy Mater.* **2011**, *1*, 63.
(15) (a) Bates, F. S.; Fredrickson, G. H. *Annu. Rev. Phys. Chem.* **1990**, *41*, 525. (b) Bates, F. S.; Fredrickson, G. H. *Phys. Today* **1999**, *52*, 32.
(16) Olsen, B. D.; Shah, M.; Ganesan, V.; Segalman, R. A. *Macromolecules* **2008**, *41*, 6809−6817.